OTC 8269

Numerical Test Tank: Simulation of Ocean Engineering Problems by Computational Fluid Dynamics

C.R. Ortloff / FMC Corporate Technology Center and M.J. Krafft / FMC SOFEC

Abstract

With the increase in knowledge in computer-based simulation methods and recent advances in high-speed computing, solutions to complex fluid-structure interaction problems, such as transient wave impact on fixed and floating structures, can now be studied in more detail. Numerical results, combined with model test measurements for verification, form the basis of the concept of the Numerical Test Tank (NTT) concept. Sample results of the application of Computational Fluid Dynamics (CFD) methods to the solution of two important ocean engineering problems are presented to illustrate the present methodology, and are then compared to model test results.

Specifically, CFD solutions are obtained for green water impact on a full-scale, FPSO hull and deck structure. The present numerical method employs a fully three-dimensional, transient, viscous Navier-Stokes solver based on the FLOW-3D/96 CFD code. The results of the simulation are shown to produce at least qualitative agreement with model test results with respect to the shape of the incident, reflected and on-deck-transient surface wave profiles. Some differences between the simulation and test results arise due to details of the simulation set-up, such as cell sizes, cell distribution, convergence criteria, turbulence model, and boundary conditions.

Additionally, CFD methods are used to compute current-force coefficients for a scale model of a 200,000 DWT tanker. Computed force coefficient values are Froude-scaled and compared to OCIMF recommendations, which are based on Froude-scaled model test data. Preliminary CFD results indicate basic agreement with OCIMF data, however future computations of coefficients for a full-scale hull, and further analysis of test data will be necessary in order to investigate viscous scale effects in more detail.

The apparent utility of the Numerical Test Tank, as illustrated by the example solutions presented, indicates that this computational approach holds promise for improving detailed knowledge of design loads for fixed and floating structures subject to severe wave and current loading.

Introduction

The design of FPSO systems for harsh wave environments often requires model testing of green water impact on deck structures. In 1993, SOFEC conducted 100-yr survival tests of the 140,000 DWT FPSO for AOPC's *Liuhua* field at MARINTEK; Figs. 1a, 1b and 1c show a typical sequence of on-deck green water flow and impact. During these tests, a limited number of instruments were used to determine impact loads on the turret surround structure and the breakwater protecting the process modules. Measured loads and volume of water which passed the breakwater were sufficiently large so as to warrant a second set of tests at MARIN (Fig. 6), specifically designed to study wave impact and breakwater optimization. In September 1996, typhoon *Sally* passed within 10 nautical miles of the *Liuhua* FPSO, generating waves (88 feet) and winds (112 knots) associated with a 200-yr event. The *Liuhua* FPSO successfully weathered this "super" typhoon with only minimal damage to pipe insulation, antennas, windows, etc.

Prediction of transient loads resulting from green water impact on FPSO hull and deck structures has traditionally been determined by scale model tests. Froude number scaling is often used to convert model test loads to full-scale values. Several potential difficulties and unknown factors may arise from this procedure, however, when applied to on-deck wave impact problems. For example, the underlying assumptions for gravity wave propagation and potential flow theory, which form the basis for prediction of Froude-scaleable wave-exciting forces on a tanker hull, are not strictly applicable for steep waves breaking on the bow, local on-deck flows, interaction of on-deck flow with deck structures or the resulting formation of air-entrained water jets.

It is generally accepted that viscous scale effects will be small near the short moments of high velocity impact, but that the post-impact flow on deck may be affected by scale. In this case, the behavior of each successive green water occurrence may be unrealistically altered by residual deck flow from the previous event, thus affecting subsequent loading. An investigation of the sensitivity of scale effects on green water impact loads is one subject in a current Joint Industry Project [1].

All of these considerations may influence the accuracy of the simple application of Froude scaling of test basin results to full-scale values. In order to study the applicability of Froude scaling, simulations were performed with FMC-developed [2] software based on the FLOW-3D/96 CFD code [3]. FLOW-3D is a three-dimensional, finite-difference, structured grid code employing SOLA-VOF [4,5,6] methods with extensive free-surface capability to solve the full, viscous Navier-Stokes equations including a variety of turbulence model choices.

Green Water Impact: Numerical and Physical Models

General research model tests on the effects of green water impact on FPSO tanker deck structures have recently been conducted at MARIN. Some of the results of these 1:60 scale model tests are given in Ref. [7]. The present study seeks to at least qualitatively compare the on-deck green water flow and impact behavior measured from these tests (Figs. 2a, 2b, 2c) to that predicted by a CFD numerical simulation of the same test conditions. As additional experimental and simulation data becomes available, more detailed comparisons can be made.

A 3-D solid model of a 160,000 DWT tanker hull was generated from the lines of a MARIN stock model using an ANSYS obstacle preprocessor [8], then transferred to FLOW-3D/96 as a fluid-flow obstacle. To ensure a hydrodynamically smooth outer-hull surface, the hull (Fig. 3a) is created with 60,000 tetrahedral elements. The entire fluid-plus-solid computational domain consists of a 600,000 active-cell mesh.

The FLOW-3D hull was next modified by adding a rectangular deck structure with height, width and location similar to the instrumented test wall. Source-code changes were also made to allow for prescription of pitching frequency and amplitude that match the motion RAO's derived from model tests. Similarly, surge and heave motions can likewise be prescribed, but were not included in the present simulation.

To approximate the regular waves employed in the model tests, the FLOW-3D code was modified to include an Airy (linear) wave train having the same height and period utilized in the tests. A few other Numerical Wave Tank studies, such as in Ref. [9], have focused on the accurate reproduction of fully non-linear wave kinematics, of which future inclusion in the present work should lead to a more accurate simulation.

Near the tanker bow, the computational grid size was refined to accommodate flow regions expected to experience sharp velocity gradients and/or free surface curvature. Additionally, the location of the wave-train generation source is sufficiently far upstream of the hull obstacle so as to eliminate reflected wave interactions with the wave source over typical wave-hull interaction times. Wave absorbing boundaries are used to eliminate reflected waves at all wave numbers at both the lateral and downstream boundaries. Finally, all CFD computations assume symmetry about a vertical half-plane coincident with the longitudinal axis of the numerical test tank.

The FLOW-3D computational model is, to a large degree, set up to duplicate key parameters of the model tests (Table 1). There are several, possibly important, differences between the model test setup and the numerical model which may limit the comparison of results to that of a qualitative nature, as the effects of some of these differences on the behavior of on-deck flow and impact could be significant. In this sense, the verification process still leaves unanswered questions related to the effects of physical as well as computational convergence, stability, finite difference solution scheme and cell size distribution parameter variations on the simulation results.

Specifically, with respect to wave-frequency vessel motions, while surge motion was restricted in the tests, both surge and heave were excluded in the simulation. The instrumented wall used in the tests more closely approximated a flat plate compared to the FLOW-3D model, which is deeper and has rounded edges. Most tests were conducted using a tanker with a flared bow, whereas the FLOW-3D hull utilized a straight profile. Finally, the deck edges were sharp for the test hull, while the FLOW-3D hull deck edges were rounded. One typical computational difficulty associated with CFD methods arises from flow around sharp edges and corners. Rounding of deck edges in FLOW-3D was implemented in consideration of obtaining more rapidly converging solutions. Future work is planned with respect to increasing the domain size so that a finer mesh can be used to accommodate the sharp deck edges.

The present FLOW-3D hull model represents the full-scale tanker. Future computations with a 1:60 scale model of same hull would, presumably, enable the numerical study of the effects of scale on green water impact pressures, forces and on-deck flow behavior.

Green Water Impact: Simulation Results

Referring to the model test photo sequences 1a,b,c and 2a,b,c, green water events can be described in three basic stages: 1) a large increase in relative wave elevation at the bow, 2) a large volume of water separates from the wave and flows aftward along the foredeck, gaining speed due to bow-up pitch accelerations, and 3) high velocity flow impacts deck structures.

FLOW-3D calculations were performed to study green water behavior at various times within a single wave cycle. First, the incident wave train is initiated three hull lengths (4.1 wave lengths) upstream of the bow; this modeling artifice allows the wave train to become uniform and establish the correct wave kinematics. One wave cycle was allowed to pass the hull before recording the green water impact sequence shown in Figs. 4a-r, which represent snapshots of fluid-hull interaction at 18 time-steps over 1.5 wave cycles. The reference frame in these figures is vessel-fixed, so that, as in the model tests with a vessel-fixed camera, the relative fluid motion is observed. Only the bow section of the hull is shown for clarity.

As can be seen, there are striking similarities between the flow behavior shown in Figs. 4a-r and that shown in the test photo sequence (Figs. 2a-c). There are also important differences which will be addressed in the following discussion.

Fig. 4a shows the initial (t=0.0s) hull and free-surface configuration prior to wave impact. Some water remains on deck from the previous cycle, which also left minor disturbances on the ocean surface. In Figs. 4b-d, the wave crest is seen to rise above the deck. At t=3-4s, pitch motion is near a maximum, and the wall of water at the bow is nearly vertical. Figs. 4e-f show a large volume of water shooting along the foredeck.

In Figs. 4d-f, one can see the distinct, two-tiered surface pattern just ahead of the bow which consists of both incident and bow-reflected wave components. This pattern is not easily seen in Fig. 2 photos because of the camera angle. However, the two-tiered surface pattern derived from FLOW-3D simulations can be compared to the centerline wave profiles (Fig. 5) measured in Ref. [7]. In addition, a photo from the *Liuhua* FPSO green water tests is provided in Fig. 6, which clearly shows excellent qualitative agreement with simulation results.

Near t=4.5s (Fig. 4f), water has contacted the deck structure, while the reflected wave pattern propagates radially outward. Also note in Figs. 4f-g that part of the incident wave flows over the side of the hull and toward the side of the deck structure. This flow behavior is not observed from the tests, and may be due in part to the exclusion of heave in the model.

By t=6.0s (Fig. 4g), the deck is completely enveloped with water. Figs. 4f-j show the impact and upward deflection of the central part of the flow on the deck structure face. In general, there appears to be a larger volume of on-deck water in the simulation than in the tests. In addition, the build-up along the centerline of the deck is thicker than is observed from Figs. 2b-c. The exclusion of heave in the simulation may again be part of the reason for these differences. Furthermore, the fine spray and splashing observed during impact in the test photos (Fig. 2c) are not well resolved in the present simulation, perhaps due to lack of refinement of the computational grid.

Figs. 4h-j show deflected water flowing off the sides of the deck, which is consistent with Fig. 2c. After the maximum water height on the deck structure is achieved, run-off of the accumulated on-deck water begins. This drainage occurs primarily near the bow quarters (Figs. 4m-p). Figs. 4q-r show the short-wave disturbances created by deck run-off, and the buildup of the next wave crest.

Although Numerical Test Tank methodology is in early stages of verification and more computational-to-test comparison work remains, qualitative comparisons with tests so far appear to indicate that the NTT method is at least promising as an alternate way to predict green water impact loads.

Prediction of Current Force Coefficients

As an additional exercise of the Numerical Test Tank method, FLOW-3D was used to predict lateral current force coefficients for a 1:82.5 scale model of a 200,000 DWT tanker. The body plan of the model hull is given in Ref. [10]. The ANSYS computer-modeled hull consists of 60,000 tetrahedral elements (Fig. 3b). Computations are made for the fully loaded vessel with a conventional bow shape at various current angles of attack and water depths. Numerical results are compared with OCIMF [11a] model tests with two different tankers sizes (190,000, 200,000 DWT), and to additional tests conducted in Ref. [10] for the same 200,000 DWT tanker. Current forces arise from a combination of pressure and viscous-shear resistance effects on the hull. Since the test model and computer model are the same size, viscous, pressure and wave drag effects should, in principal, be the same.

For the present study, a uniform current with a velocity of 1.0m/s was prescribed. The mean surface current velocity in the model tests ranged from 1.03-2.06m/s. Ref. [10] performed a sensitivity study with respect to velocity, and concluded that force coefficients were essentially velocity-independent over a typical range (1.0-2.5m/s). In both the experiments and computations, lateral force coefficients, C_Y, are obtained by dividing the measured or predicted mean force by a constant factor $K=\frac{1}{2}\rho V_c^2 L_{bp} T$, where ρ, L_{bp}, and T are seawater density, length between perpendiculars and draft, respectively. V_c is the depth-averaged velocity over the draft of the tanker.

Lateral force coefficients obtained from FLOW-3D simulations and OCIMF tests are compared in Fig. 7 for various water-depth-to-draft ratios (*WD/T*) and current angles of attack (stern-on is zero degrees). FLOW-3D computations were performed for *WD/T* ratios of 1.4, 4.4 and >6.0 for angles of attack of 45, 90 and 135 degrees. As shown in Fig. 7, there is reasonable agreement between computations and OCIMF data. In general, as *WD/T* ratios decrease, the predicted C_Y are increasingly overestimated compared to OCIMF, particularly for the largest relative current attack angle of 90 degrees. The computed C_Y for *WD/T*=16.0 is somewhat lower than for OCIMF for *WD/T*=6.0; OCIMF suggests that *WD/T*=6.0 is the deep water limit, above which there is no change in C_Y.

That the CFD-predicted force coefficients are somewhat higher than the published OCIMF data for the smaller *WD/T* ratios is consistent with observations made during the model tests. In Ref. [11b] it is noted that tests with small *WD/T* ratios and quartering to beam-on current experienced vortex shedding around the ends of the vessel. As the model scale decreased (decreased Reynolds number), both the observed vortex shedding and the drag coefficient increased. Because the prototype Reynolds number is two orders of magnitude greater than for the model scale, little or no vortex shedding is expected for the prototype. Vortex shedding components of the current force were then estimated from the force time-histories and subtracted out before computation of the mean force coefficient data given in Refs. [11a,11b]. No such adjustment has been made for the FLOW-3D coefficients. Instead, future computations for a full-scale hull are planned for the purpose of evaluating the magnitude of these viscous scale effects.

Given current practical run time limitations, it is important to describe a few key numerical artifices that are available to help obtain meaningful flow solutions in reasonable computational times (usually >>200 cpu-hrs on Pentium-Pro systems). The lateral and downstream CFD boundary conditions will encounter starting transients from the initiation of current, waves generated by steady flow past the hull, and disturbances due to potential periodic wake-shedding around the ends of the hull. Therefore, to absorb this energy, sufficient damping must be introduced via viscosity and turbulence models.

Additionally, energy-absorbent boundaries in the form of inclined, porous ramps and/or sink obstacles are also useful for obtaining steady-state solutions in compact computational domains. These considerations apply when domain size is limited by economics. If the domain is sufficiently increased (say, to the order of several million cells, compared to 600,000 for the present model), then reflections at far-field boundaries will not occur until after "steady-state" conditions are established.

Although the present simulation includes internal and boundary damping mechanisms, the force time-histories still have some unavoidable small-amplitude, low-frequency oscillations, even after 1,500 hours of real-time simulation. These fluctuations, coupled with vortex shedding transients, prevent one from obtaining a truly steady solution. Therefore, results in Fig. 7 represent "best-estimate" mean values. Ideally, in the absence of vorticies, if sufficient cells are available, then a critical cell size exists below which forces remain constant.

The adequacy of the current computer simulation is shown, but there are some indications that suggest more refinement in flow stability criteria related to cell size and other key geometric and physical parameters, together with improvement in wave damping boundary conditions, are necessary to ensure high accuracy solutions in limited computational domains. The results shown are, therefore, to be regarded as preliminary.

Summary

The apparent utility of the Numerical Test Tank concept, as illustrated by the example solutions presented, indicates that this computational approach holds promise for improving detailed knowledge of design loads for a variety of offshore structures subject to severe wave and current loading, such as fixed platforms, TLP's, Semi's and Spar's. The present NTT method is currently in an early stage of development awaiting further improvements in theoretical and numerical solution techniques, as well as additional test verification.

Results of the two sample analyses presented indicate the ability of CFD methods to provide supplemental information to scale-model testing. In some cases, 3-D computations can provide insight into details of the flow field not usually available from tests due to the technical limitations of test probes and the limited number of placements available in a flow field; in this sense, force, pressure, velocity, etc., are available at all computational nodes, rather than a few test probe locations. NTT methods also have the potential to provide accurate full-scale predictions without reliance upon scaling parameters.

NTT methods also have the potential to identify scale parameters for conversion of test data to prototype results. For some complex fluid-structure interactions, it is difficult to experimentally assess scale effects. Since the NTT approach can provide solutions for both model and full-scale structures, the differences in results can be determined.

References

1 "JIP F(P)SO Green Water Loading", MARIN Proposal No. 2.13644, Maritime Research Institute Netherlands, Wageningen, Netherlands, Apr 1996.

2 Ortloff, C.R., FPSO Green Water Interaction and Load Prediction Methodology by CFD Methods, FMC Corporate Technology Center Report 7024, Santa Clara, CA, Sept. 1995.

3 Hirt, C.W., FLOW-3D Quick Reference Guide, Ver. 7.0, Flow Science, Inc., Los Alamos, New Mexico, 1995.

4 Hirt, C.W. and Nichols, B.D., "Volume of Fluid Method for the Dynamics of Free Boundaries", *J Comp Phy* 39, Vol 201, 1981.

5 Sicilian, J.M., and Hirt, C.W., HYDR-3D, A Solution Algorithm for Transient 3-D Flows, Flow Science, Inc., Los Alamos, NM, 1985.

6 Hirt, C.W., Amsdem, A.A. And Cook, J.L., "An Arbitrary Lagrangian-Eulerian Computing Method for all Flow Speeds", *J Comp Phy* 14, Vol 227, 1974.

7 Buchner, B., "The Impact of Green Water on FPSO Design", *Proc 26th Offshore Tech Conf*, No 7698, Houston, May 1995.

8 ANSYS Users' Manual, Swanson Analysis Systems, Inc., Rev. 5.0, Houston, PA, 1992.

9 Boo, S.Y., Kim, C.H. and Kim, M.H. "A Numerical Wave Tank for Nonlinear Irregular Waves by 3-D Higher Order Boundary Element Method," *Int J Offshore and Polar Eng*, Vol 4, No 4, Dec 1994.

10 Wichers, J.E.W., A Simulation Model for a Single Point Moored Tanker, Maritime Research Institute Netherlands Report 797, Wageningen, Netherlands, June 1988.

11a Oil Companies International Marine Forum (OCIMF), Prediction of Wind and Current Loads on VLCC's, 2nd Edition, Witherby and Co., London, 1994.

11b Oil Companies International Marine Forum (OCIMF), Prediction of Wind and Current Loads on VLCC's, 1st Edition, Witherby and Co., London, 1977.

Acknowledgments

The authors wish to thank Mr. B. Buchner of MARIN for his comments and suggestions on model test verification methods, and for contributing Figs. 2 and 5.

Table 1 Comparison of FLOW-3D model with test setup for 160,000 DWT FPSO (full scale).

	TESTS	FLOW-3D
3-DOF vessel wave-frequency motions		
Pitch	Yes	Yes
Heave	Yes	No
Surge	No	No
Environmental particulars		
Water Depth	150 m	150 m
Wave Type	Regular	Airy
Wave Height / Period	17.3 m / 11.20s	17.3 m / 11.00s
Current Velocity	0.00 m/sec	0.00 m/sec
Vessel particulars		
Hull Length	260.34 m	260.34 m
Hull Beam	47.10 m	47.10 m
Hull Draft	17.52 m	17.52 m
Freeboard	8.88 m	8.88 m
VKG	14.22 m	14.22 m
LCG from Midship	6.72 m	6 .72 m
Bow Flare	Yes	No
Hull Contour Match	Yes	Yes
Deck Edges	Sharp	Rounded

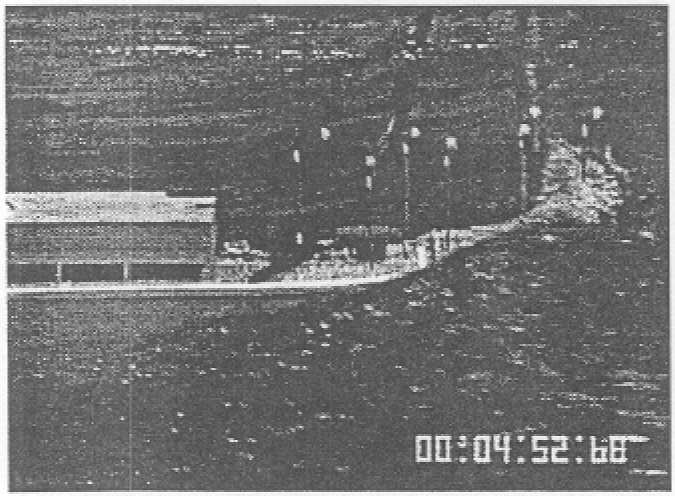

Fig. 1a AOPC Liuhua FPSO survival test (MARINTEK): photo A.

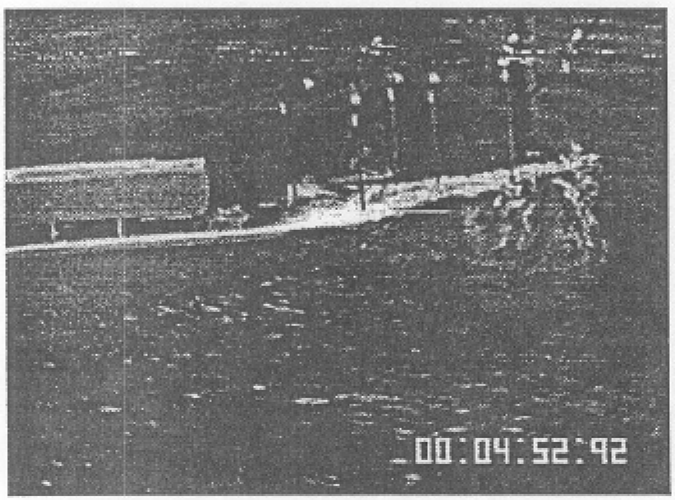

Fig. 1b AOPC Liuhua FPSO survival test (MARINTEK): photo B.

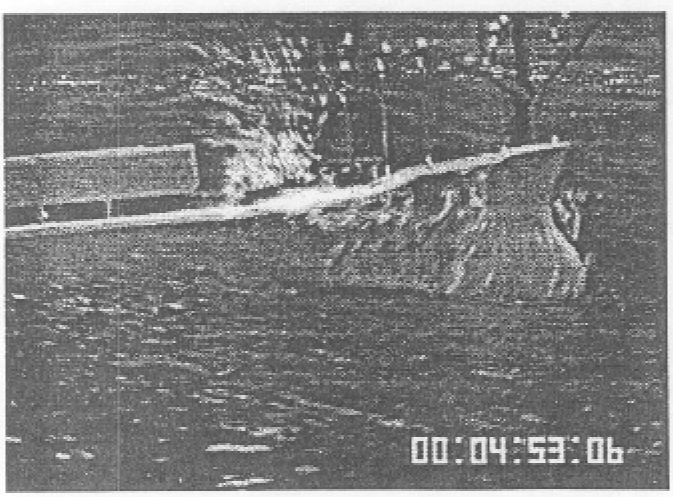

Fig. 1c AOPC Liuhua FPSO survival test (MARINTEK): photo C.

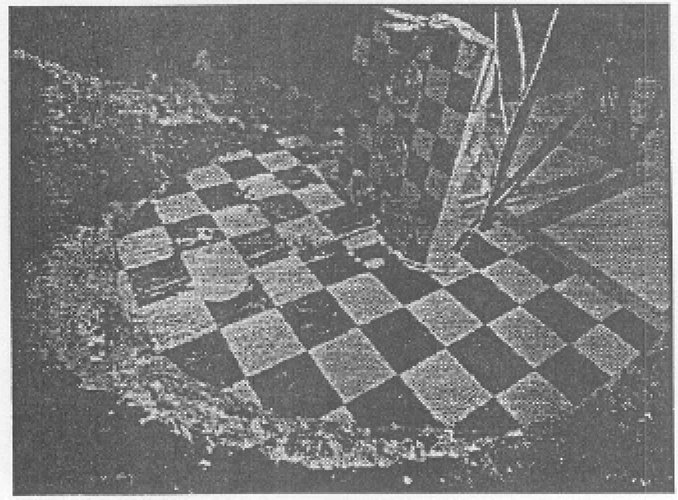

Fig. 2a MARIN green water research test [ref. 7]: photo A.

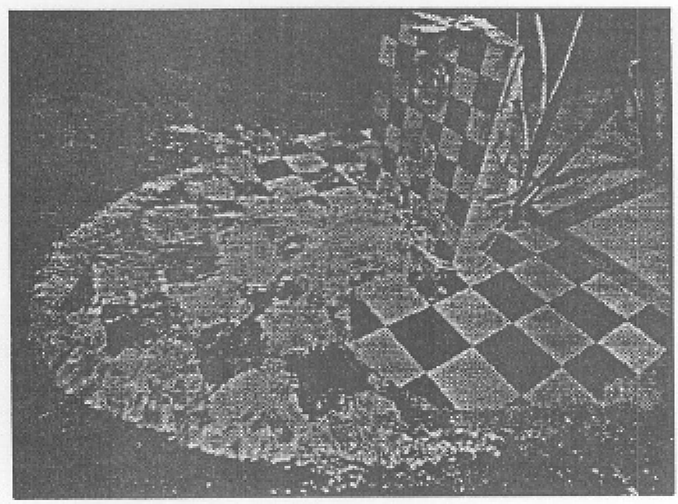

Fig. 2b MARIN green water research test [ref. 7]: photo B.

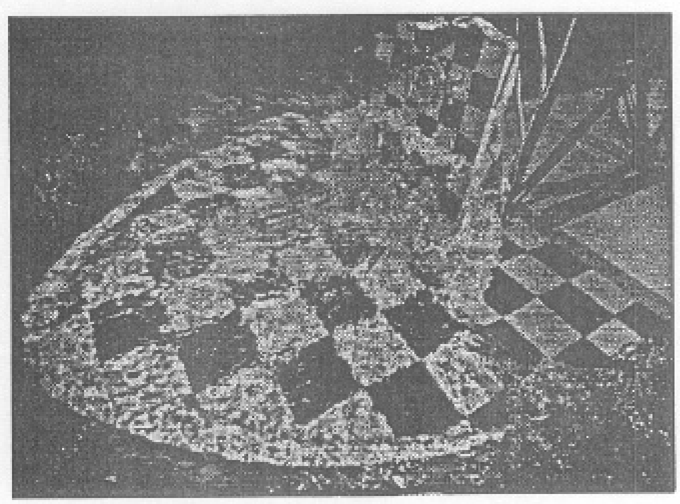

Fig. 2c MARIN green water research test [ref. 7]: photo C.

160,000 DWT Tanker

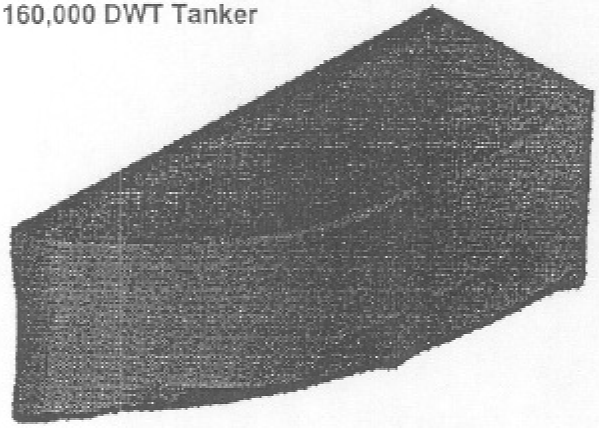

Fig. 3a ANSYS hull model for green water impact study (only port side of forward portion of vessel shown for clarity).

200,000 DWT Tanker

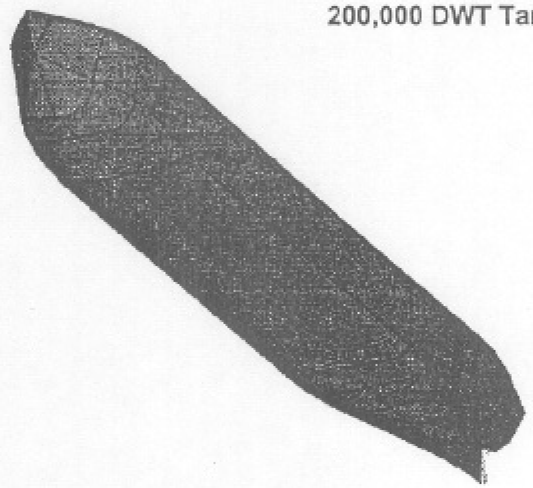

Fig. 3b ANSYS hull model for current force coefficients study.

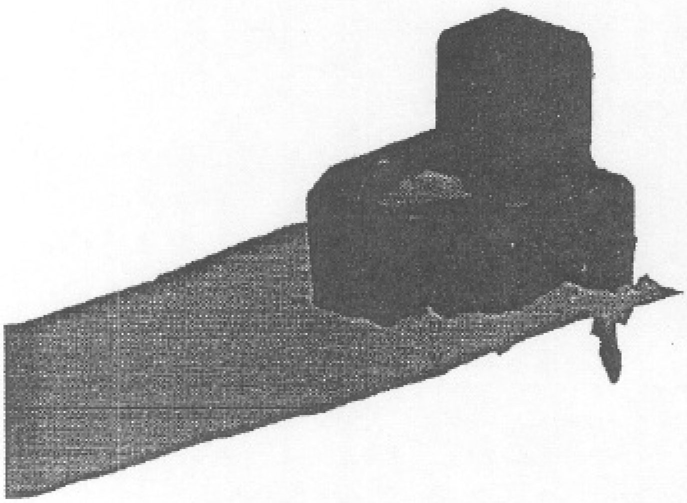

Fig. 4a FLOW-3D simulation: time = 0.0 sec.

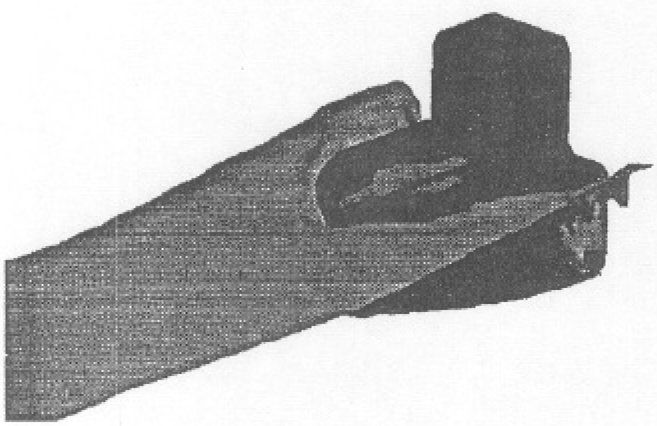

Fig. 4b FLOW-3D simulation: time = 1.0 sec.

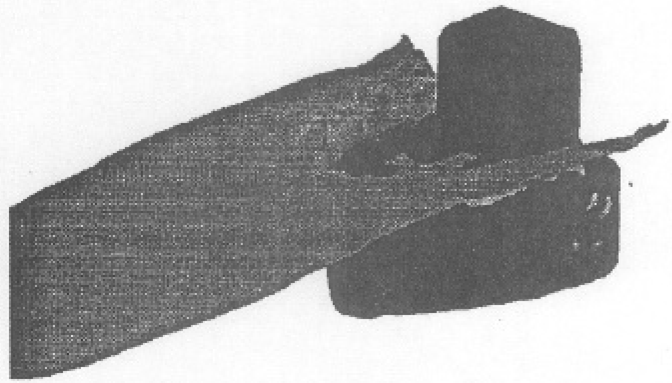

Fig. 4c FLOW-3D simulation: time = 2.5 sec.

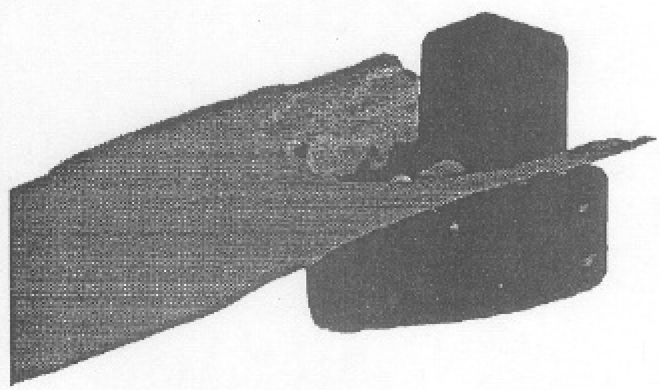

Fig. 4d FLOW-3D simulation: time = 3.5 sec.

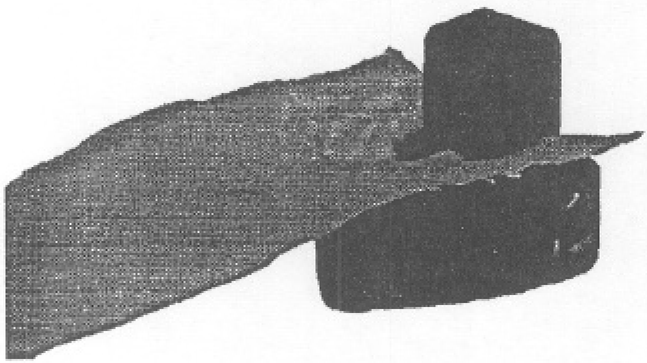

Fig. 4e FLOW-3D simulation: time = 4.0 sec.

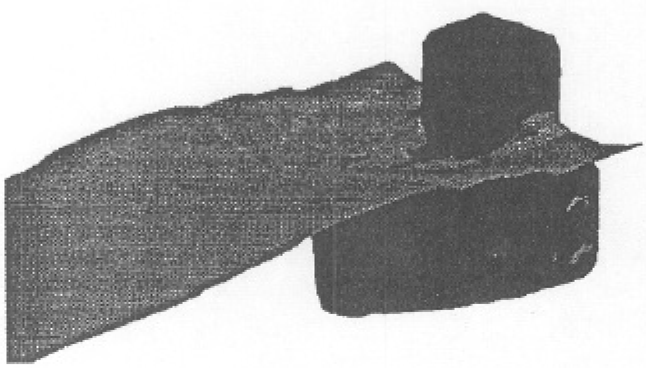

Fig. 4f FLOW-3D simulation: time = 4.5 sec.

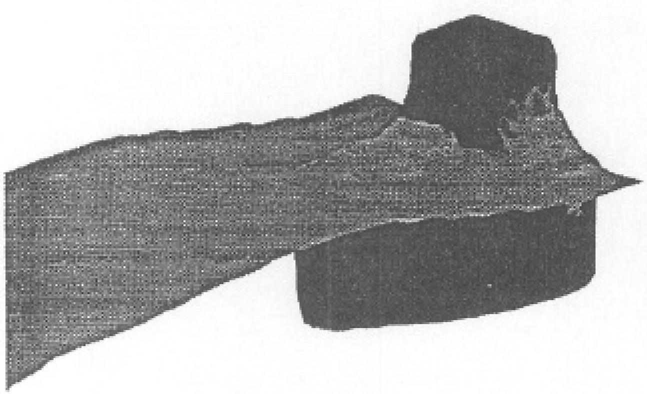

Fig. 4g FLOW-3D simulation: time = 6.0 sec.

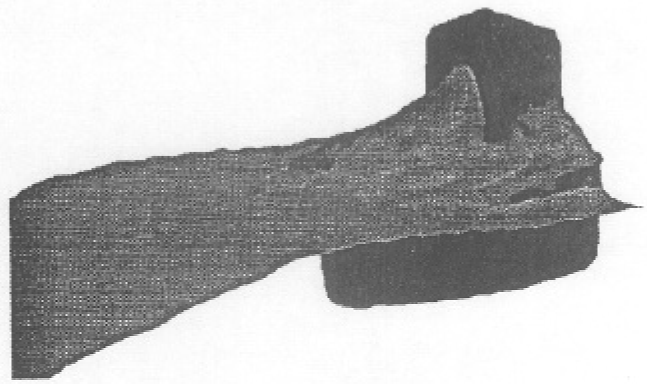

Fig. 4h FLOW-3D simulation: time = 7.0 sec.

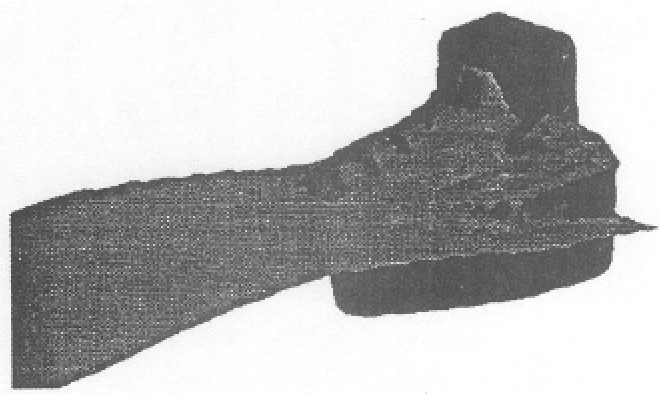

Fig. 4i FLOW-3D simulation: time = 8.0 sec.

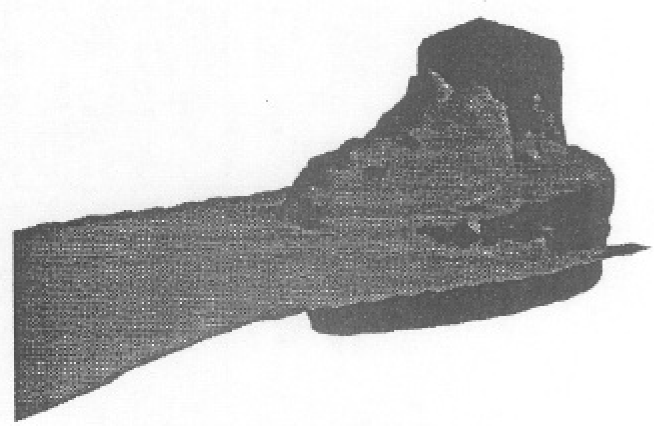

Fig. 4j FLOW-3D simulation: time = 8.5 sec.

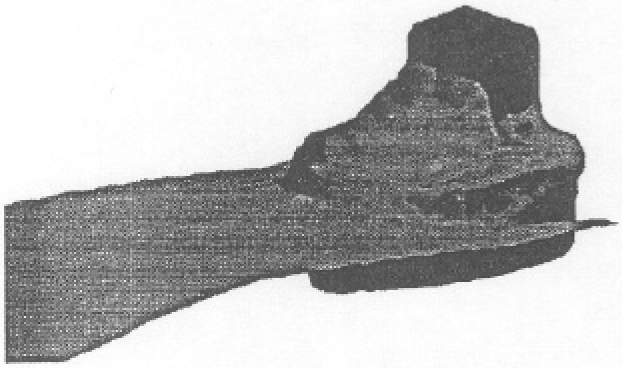

Fig. 4k FLOW-3D simulation: time = 9.0 sec.

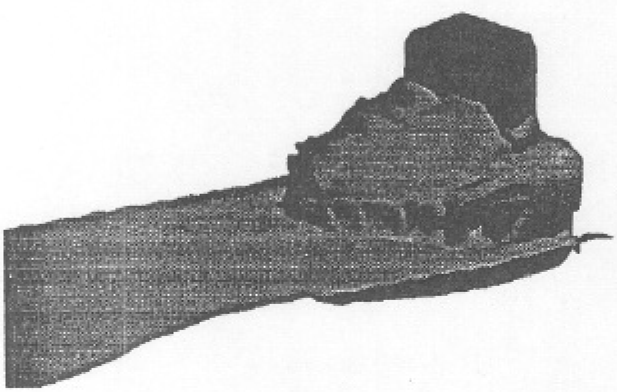

Fig. 4l FLOW-3D simulation: time = 10.0 sec.

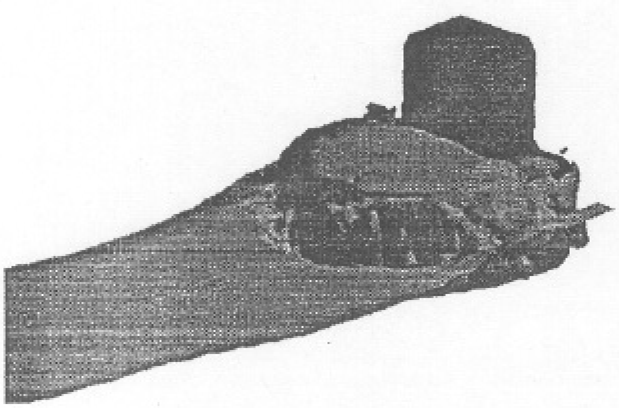

Fig. 4m FLOW-3D simulation: time = 10.5 sec.

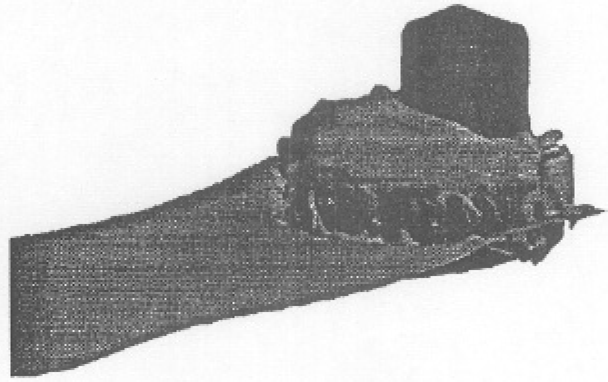

Fig. 4n FLOW-3D simulation: time = 11.0 sec.

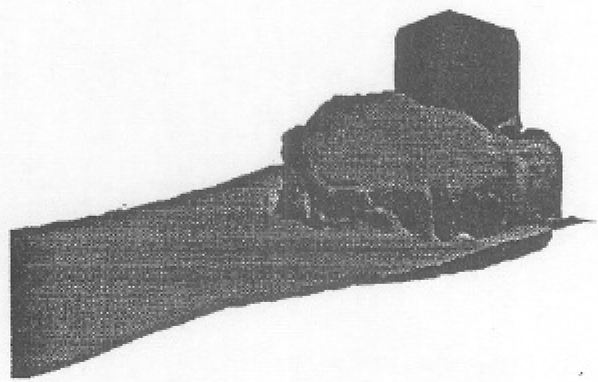

Fig. 4o FLOW-3D simulation: time = 11.5 sec.

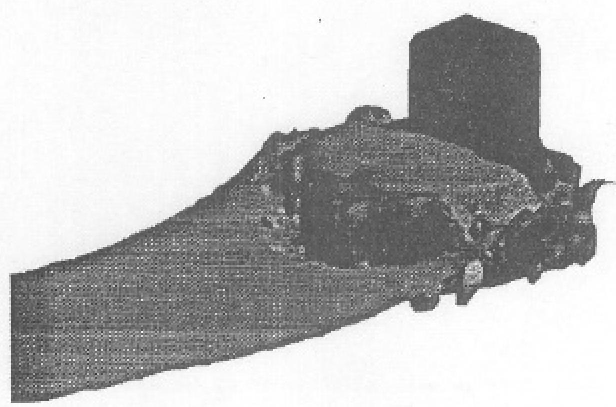

Fig. 4p FLOW-3D simulation: time = 13.0 sec.

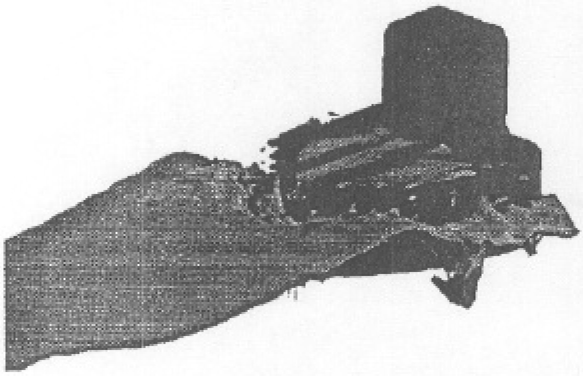

Fig. 4q FLOW-3D simulation: time = 14.5 sec.

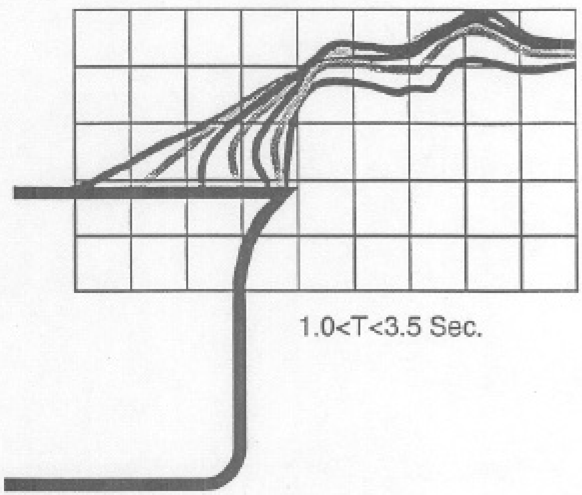

Fig. 5 Centerline wave profiles (0.25s intervals): MARIN test 4482.

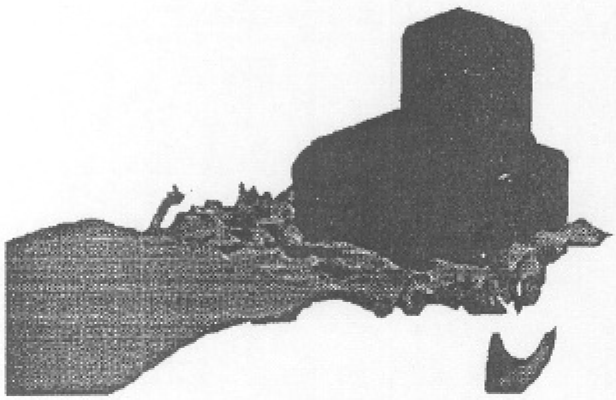

Fig. 4r FLOW-3D simulation: time = 17.0 sec.

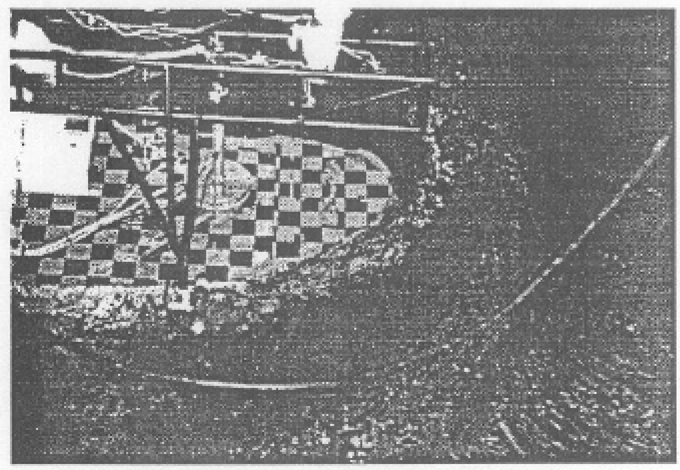

Fig. 6 AOPC Liuhua FPSO green water model test (MARIN).

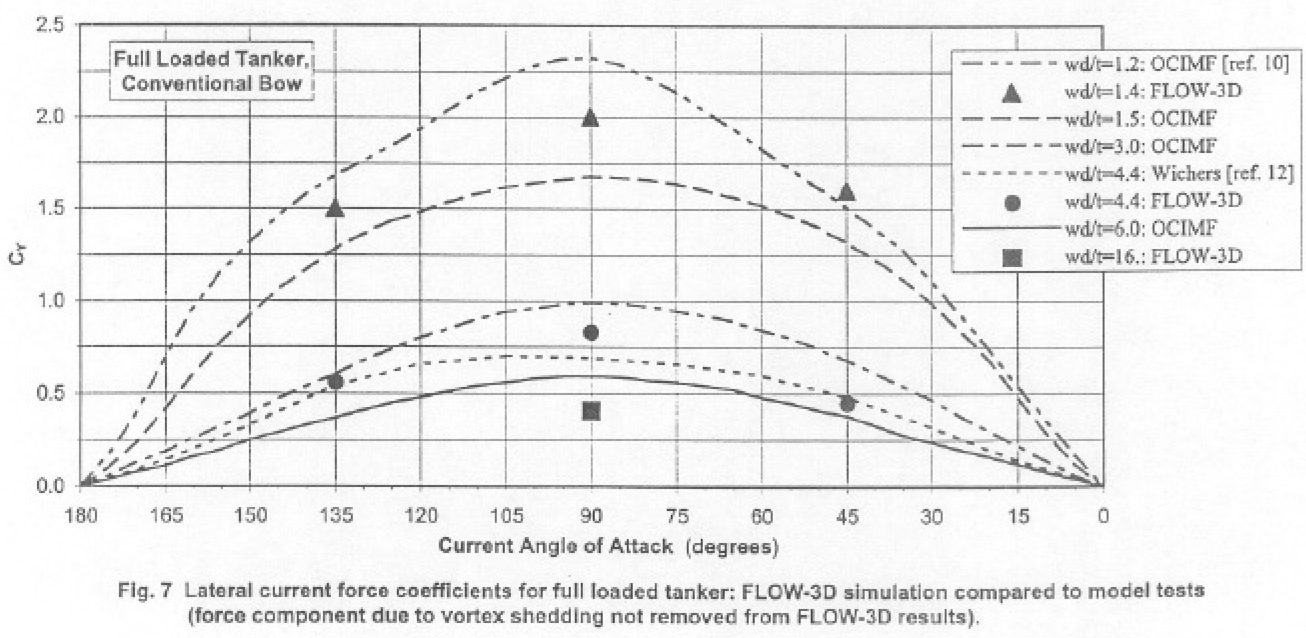

Fig. 7 Lateral current force coefficients for full loaded tanker: FLOW-3D simulation compared to model tests (force component due to vortex shedding not removed from FLOW-3D results).